Response to reviewer's comments (RC1)
Spatiotemporal heterogeneity in the increase of ocean acidity extremes in the Northeast Pacific

Flora Desmet, Matthias Münnich, and Nicolas Gruber

October 26, 2023

General remarks

First and foremost, we thank the editor and this reviewer for their very supportive and insightful comments on our manuscript. We appreciate the valuable remarks that helped us to significantly improve the quality of this manuscript.

Many of the reviewer's comments center on two issues: (i) the comparison of the modeled subsurface fields with observations, and (ii) the role of changes in $[H^+]$ variability on the increase of OAX. In response to (i), we added an evaluation of the simulated subsurface trends in dissolved inorganic carbon using observations from a repeat transect to station "P" in the Northeast Pacific. In response to (ii), we added a discussion paragraph on the contribution of changes in $[H^+]$ variability to OAX increase together with an additional appendix figure. Based on the reviewer's comments, we also clarified the role and impact of the southern boundary of the model. In addition to the responses to the reviewer's comments, we updated a few numbers, due to our recent noticing that we had used an improper area weighting of spatial averages in our initial submission. These updates are very minor and have no implications for the key findings and messages of the manuscript.

Herein, we provide a summary of each of the reviewer's comments (RC1) in black, followed by our point by point replies in blue and the text added or changed in the revised manuscript in red.

Specific replies

Reply to Reviewer's comments (RC1):

General Comments

The authors provide an informative and insightful analysis of ocean acidification extreme events (OAX) in the North Pacific. They demonstrate the skill of their model in simulating observed OA trends, and they have addressed its representation of mean conditions and variability in a previous study (Desmet et al, 2022). They highlight the regional heterogeneity in frequency and intensity of extreme conditions in a changing climate and point out the processes contributing to regional differences, such as the magnitude of regional variability relative to the long-term trend and the influence of off-shore propagating eddies on property distributions. Additionally, they attribute changing OAX conditions to CO2 increase by comparing to a control simulation based on 1979 conditions. Their analysis of the role of mesoscale eddies in driving regional OAX characteristics is particularly interesting.

Authors: We thank the reviewer for the very supportive comments.

Specific Comments

1) It appears that the model-observation comparisons are made only with surface data. Since an analysis of conditions at depths of up to 250 m is one of the interesting aspects of this study, could the authors provide some evaluation/discussion of model skill at these depths?

Authors: We thank the reviewer for this valuable comment and agree that an evaluation of modeled subsurface OA trends is warranted. However, only a very limited evaluation is possible due to the lack of long-term subsurface observations. The only long-term observations of the marine carbonate system at depth known to us stem from line P based on the work of Franco et al. [2021]. Unfortunately, their analysis is limited to DIC. Still, this is clearly of value. Thus, we added an evaluation of our modeled subsurface DIC trends against these observation-based trends.
The modeled DIC trends (DIC is normalized to a salinity value of 33 psu) are overall well confirmed by the observations, but the model tends to have higher trends than suggested by the observations (Figure 1). Even though there are substantial uncertainties associated with the observation-derived trends, this discrepancy needs to be noted. We discuss the implications of this finding in the caveat section of the revised manuscript. If it holds up to further scrutiny, this model bias would imply a slower increase of the sub-surface OAX than simulated, but no change in our conclusions about the abruptness of the onset of the OAX or the large spatial heterogeneity.

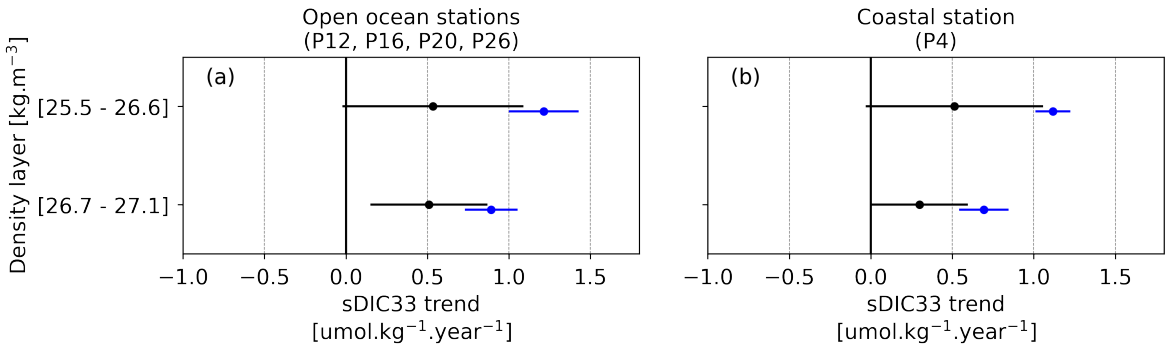

Figure 1: Appendix Figure B2 in revised manuscript: Trends in dissolved inorganic carbon normalized to a salinity value of 33 psu (sDIC33) in the subsurface of line P (in μmol kg^{-1} year^{-1}). (blue) Simulated ROMS-BEC trends and (black) observed trends from Figure 6 in Franco et al. [2021]. The trends have been averaged within two density layers, namely mixed layer/pycnocline waters ([25.5 - 26.6] kg m^{-3}) and intermediate waters ([26.7 - 27.1] kg m^{-3}), as well as across the four open ocean stations (P12, P16, P20, P26) in panel (a). Black error bars denote the average of the two standard deviation credible interval (95% CrI) of individual data points from Figure 6 in Franco et al. [2021], while blue error bars denote the spatial standard deviation across stations and density levels from ROMS-BEC simulated trends.

In response to this comment, we included Figure 1 in the appendix of the revised manuscript. In the revised manuscript, we modified the model evaluation section as follows:

Text added:

Lines 153-161: "While the evaluation of subsurface pH and Ω_A trends is not yet possible given the lack of long-term time series observations, we evaluate the simulated subsurface trends in dissolved inorganic carbon down to about 300 m depth against observations derived from the line P time series [Appendix Figure B2; Franco et al., 2021]. The simulated dissolved inorganic carbon trends (DIC is normalized to a salinity of 33 psu) in the subsurface of line P stations are in the range of observed trends (Appendix Figure B2). However, the model tends to have larger trends than suggested by the observations. In intermediate waters (150-300 m depth), simulated DIC trends are 2% larger than the upper bound of observed trends in open ocean stations, and 15% larger in the coastal station P4 (Appendix Figure B2). We further discuss the implications of this discrepancy in the caveat section

4.4.
Overall, although subsurface trends in dissolved inorganic carbon tend to be overestimated, our model simulates [...]"

We additionally discuss the implications of this evaluation in the caveat section of the revised manuscript as follows:

Lines 494-501: "The use of relative thresholds on fixed baselines to define OAX requires the model to accurately capture OA trends since the ratio of the long-term trend to local variability is key in determining the increase in OAX in that case. Giving us confidence in our results are the well captured pH and Ω_A surface trends over the last four decades by our model. Yet, in the subsurface, simulated dissolved inorganic carbon trends tend to be higher than suggested by observations, even though substantial uncertainties associated with the observation-derived trends exist [Franco et al., 2021]. If this model subsurface bias holds up to further scrutiny and for other carbonate variables such as $[H^+]$, it would imply a slower increase of subsurface OAX than simulated. Yet our conclusions about the large spatial heterogeneity in the progression of OAX and the abruptness of the onset of the OAX in the far offshore regions would remain unchanged."

Besides, as stated in the general comments of the reviewer, we addressed the model representation of the mean conditions of key variables at depth (Figures 2 and 3), as well as the representation of the depth distribution of pH and Ω_A during the North American Carbon Program West Coast Cruise [Feely et al., 2008] (Figure4) in a previous study [Desmet et al., 2022]. The HCast simulation in our manuscript uses the same model configuration and forcing as employed by Desmet et al. [2022]. There were some small changes owing to our use of slightly different initial conditions as a result of a change in the forcing used for the model spin up. While Desmet et al. [2022] used daily fields from the year 1979 as the forcing for the spin up, we use a normal year forcing (apart from atmospheric CO_2, which is transient). The normal year forcing is created by adding daily anomalies of the year 2001 to the climatological mean surface fields of wind stress, short and long-wave radiations, and freshwater fluxes derived from ERA-5 [Hersbach et al., 2020; Copernicus Climate Change Service (C3S), 2017]. The two simulations are therefore not numerically equivalent, but present very similar evaluation results (cf. Figures 2, 3, and 4, and Desmet et al. [2022]).
We address this by adding the following sentences in the methods of the revised manuscript:

Text added:

Lines 115-120: "Our HCast simulation uses slightly different initial conditions than employed by Desmet et al. [2022] as a result of a change in the forcing used for the model spin up. While Desmet et al. [2022] used daily fields from the year 1979 as the forcing for the spin up, we use a normal year forcing (apart from atmospheric CO_2, which is transient). The normal year forcing is created by adding daily anomalies of the year 2001 to the climatological mean surface fields of wind stress, short and long-wave radiations, and freshwater fluxes derived from ERA-5 [Hersbach et al., 2020; Copernicus Climate Change Service (C3S), 2017]."

Lines 138-140: "Although our HCast simulation is not numerically equivalent to the simulation employed by Desmet et al. [2022] owing to the different initial conditions (cf. Section 2.1), they present very similar evaluation results (not shown). Here we further evaluate the surface OA trends in pH and Ω_A of the model against observations (Table 1)."

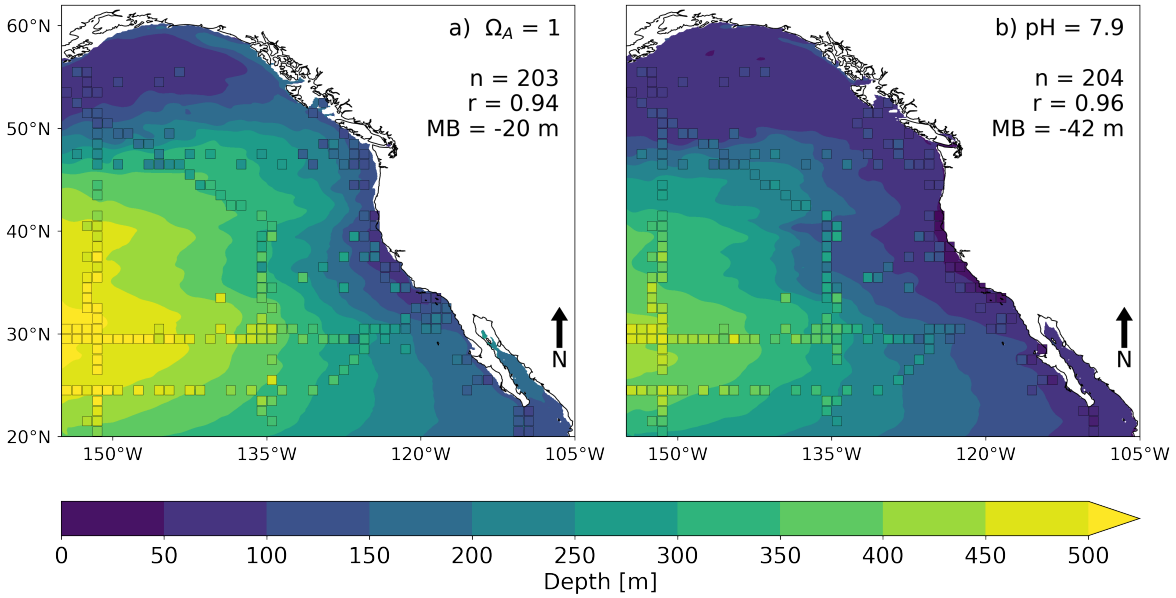

Figure 2: Evaluation of the model (HCast) simulated annual mean depths of (a) the Ω_A saturation horizon (Ω_A=1) and (b) the pH = 7.9 isosurface compared to the corresponding observational estimates based on the 1°×1° gridded GLODAPv2 climatology [Lauvset et al., 2016]. The model simulated results are shown as filled contours, while the (gridded but not mapped) observations are shown as filled squares. Each square stands for the corresponding 1°×1° bin of the gridded product. The corresponding spatial Spearman's correlations (r), spatial mean biases (MB), and number of points (n) used for the calculation are indicated at the top.

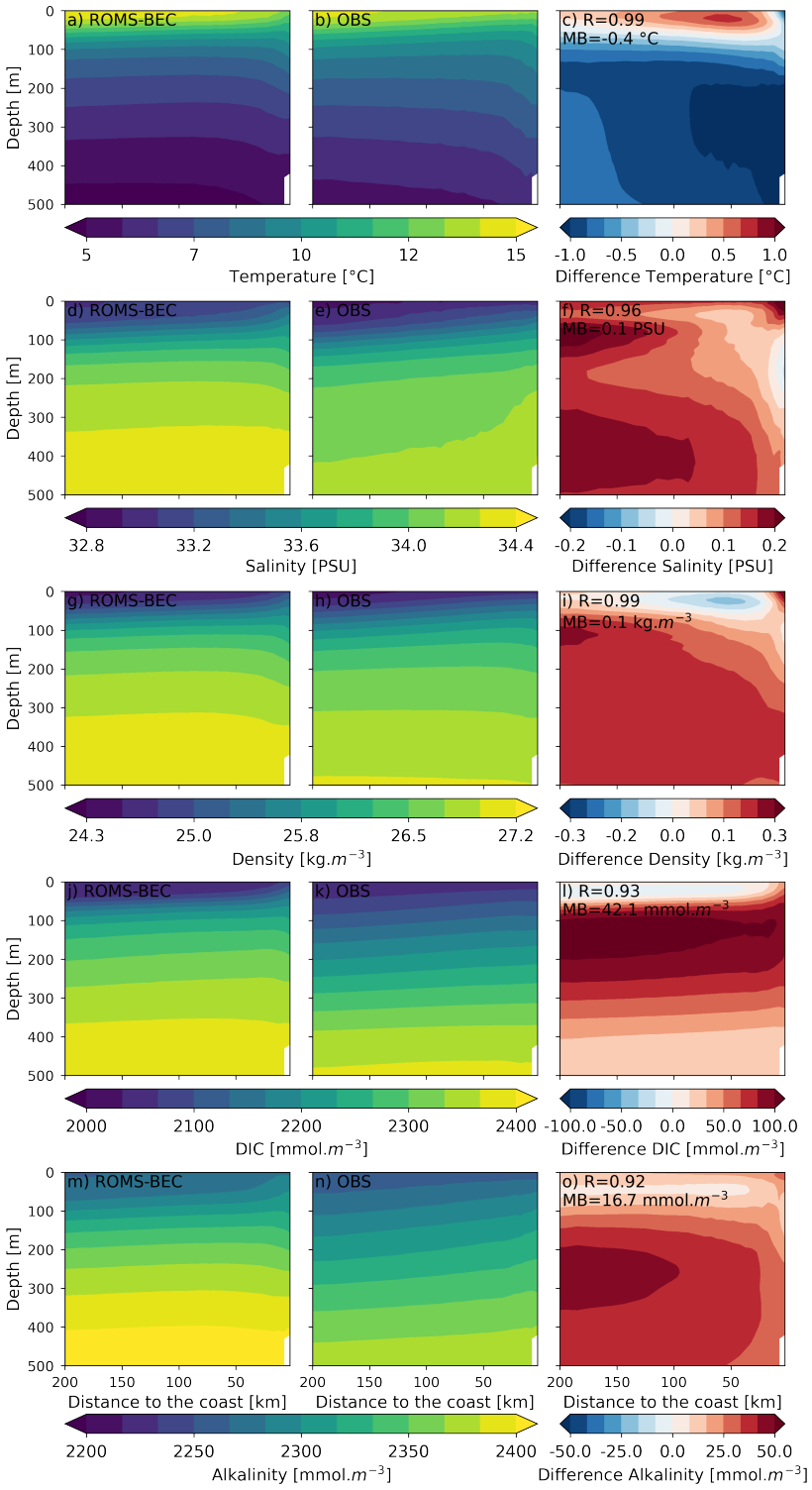

Figure 3: Climatological mean (1984-2019) interior temperature (a-c), salinity (d-f), density (g-i), DIC (j-l) and alkalinity (m-o) in ROMS-BEC (HCast) are evaluated against SODA 1.4.2 [Carton and Giese, 2008] for the temperature, salinity and density, and 1°x1°GLODAPv2 gridded datasets [Lauvset et al., 2016] for DIC and Alkalinity. Spatial correlation (R) and mean bias (MB) are given in each differences plot. Cross-section is averaged over the region denoted by the black contour line in Figure 5a in Desmet et al. [2022] until 200 km from the coast and 500 m depth.

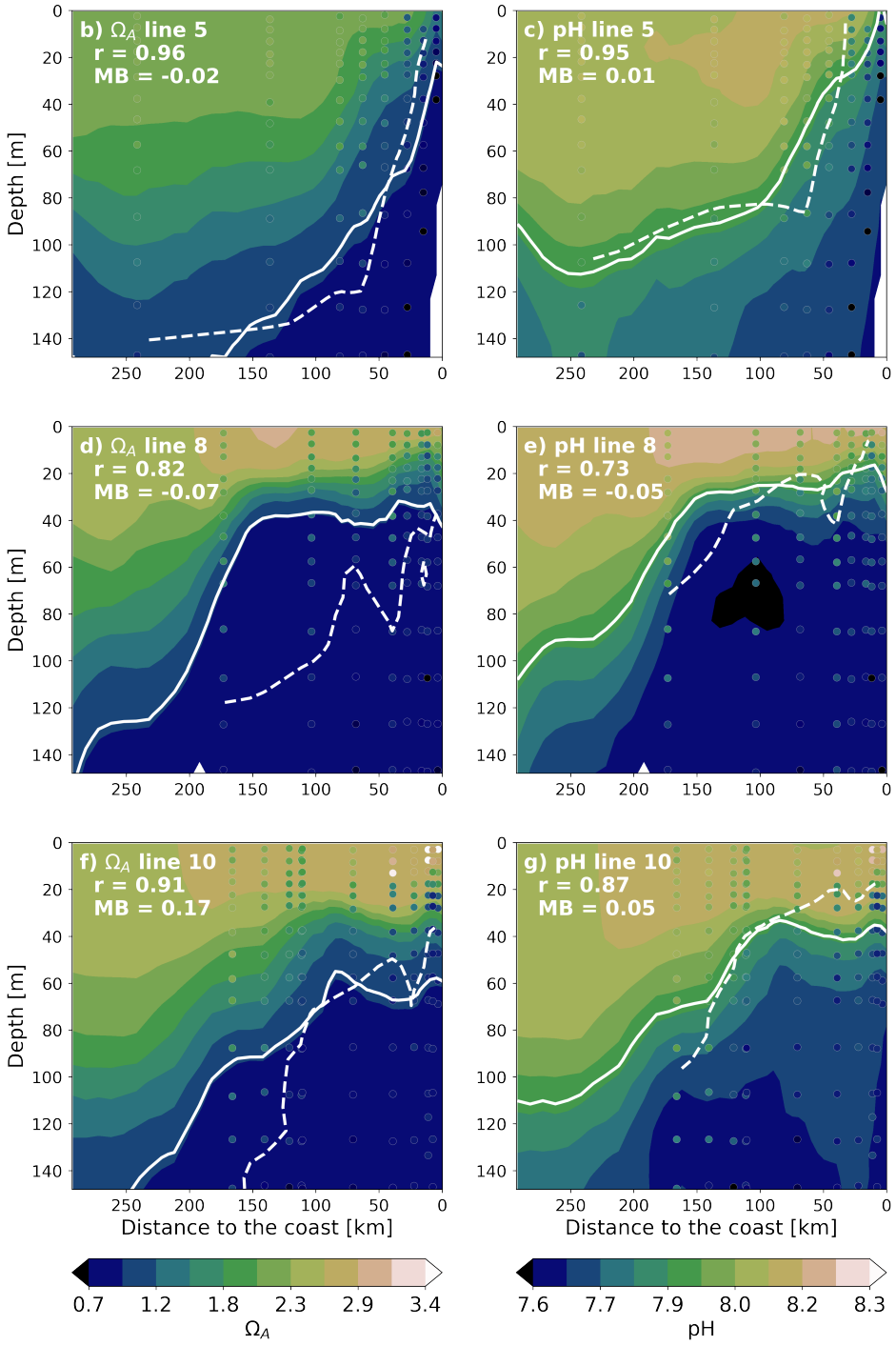

Figure 4: Evaluation of model (HCast) simulated Ω_A and pH against observations from the North American Carbon Program (NACP) West Coast Cruise [Feely et al., 2008]. (a) Map of stations and masks used for simulated fields for each transect, plotted on top of every fifth grid lines of ROMS-BEC grid. (b–g) Offshore transects of (b, d, and f) Ω_A and (c, e, and g) pH at transect 5 (top), 8 (middle), and 10 (bottom) (see map in Figure 2a of Desmet et al. [2022] for locations). The model simulated fields are shown as filled contours, while the observations are shown as filled circles. White lines denote the simulated (solid lines) and observed (dashed) $\Omega_A = 1$ horizon (b, d, and f) and $pH_{7.9}$ isopleth (c, e, and g), respectively. Spearman spatial correlations (r) and mean biases (MB) between model and observations of the interior distribution along those transects are given in the top left corners.

2) Please include some discussion of the altered southern boundary condition in the control run in the context of attribution of OAX events to the rise in atmospheric CO2. How large is the impact of the southern boundary DIC concentration relative to gas exchange within the domain?

Authors: We thank the reviewer for raising this issue. Since the southern lateral boundary of the model is nearly 10 000 km away from the domain used for the analysis, i.e., almost at the antipode of the CCS (Figure 5b), the influence of DIC change at the lateral boundaries on the detected OAX relative to gas exchange is negligible. It is not only the distance, but also the presence of the equator, which forms a strong natural barrier for inter-hemispheric exchange, that prevents signals from the southern boundary to influence our results. Please note that this issue is actually the reason why we opted for such a large domain in the first place, rather than using a regular grid whose domain is smaller, which makes the influence of the lateral boundary conditions much more substantial.

To better reflect the remote position of the southern boundary condition relative to the domain of analysis, we included in Figure 1 of the revised manuscript an additional panel (b) showing the entire telescopic grid and where the position of the southern boundary condition can be seen (Figure 5).

Text added:

Line 110: "[...] except at a few places in the Southern Ocean, i.e., more than 9000 kilometers away from the analysis domain."

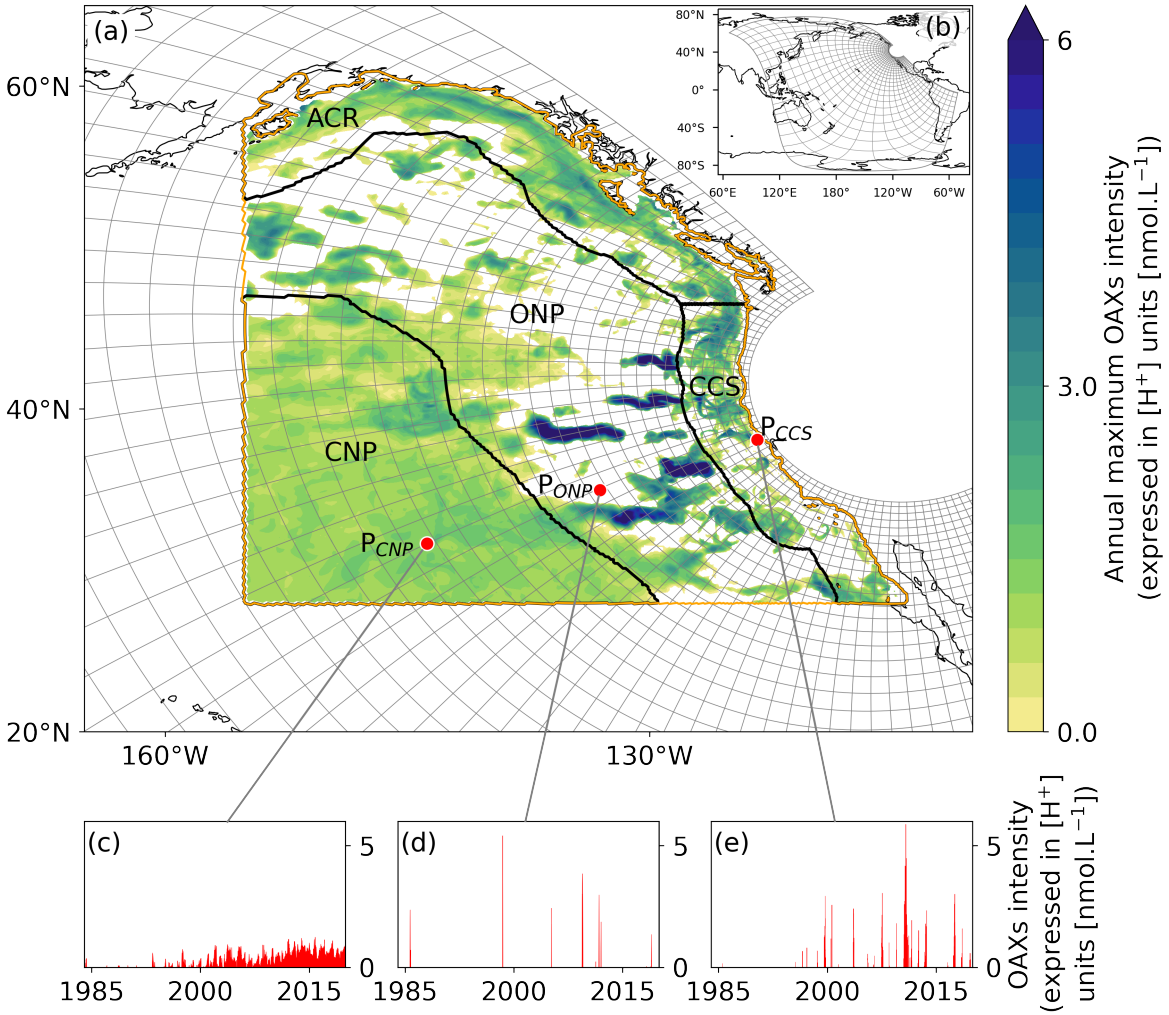

Figure 5: Map of the analysis domain and the selected subregions, and key properties of the diagnosed OAX. (a) Map of the Northeast Pacific with the telescopic grid of the model plotted in grey for every 10^{th} grid cell. The black contours delimit the four selected subregions, i.e., the two coastal regions inshore of 300 km, namely the Alaskan Coastal Region (ACR) and the California Current System (CCS), and the two open ocean regions, i.e., the Offshore Northeast Pacific (ONP) and the Central Northeast Pacific (CNP). The domain of analysis is denoted by the orange contour line. The annual maximum intensity of the simulated OAXs in year 2014 at 100 m depth is plotted on top. White regions indicate that no OAX occurred in that year at this depth. (b) Map of the whole ROMS-BEC telescopic grid, plotted for every 20^{th} grid cell. (c-e) Time series of $[H^+]$ intensity at 100 m depth at the three locations depicted by red points in (a), i.e., (left) P_{CNP} in the CNP region (31.66°N-143.77°W), (middle) P_{ONP} in the ONP region (34.97°N-133.07°W), and (right) P_{CCS} in the CCS (38.08°N-123.32°W).

Is the removed trend in DIC fully attributable to atmospheric CO2 increase or could there be a contribution associated with interannual variability?

Authors: We thank the reviewer for this relevant question. First of all, we would like to refer to the answer to the previous comment in that the exact nature of these Southern Ocean boundary conditions have a negligible impact on our study region. We still paid attention to these boundary condition, since we are using this simulation also for studies elsewhere in the Pacific. Thus onward to the specific question raised by the reviewer: Yes, the removed trend in the Southern Ocean DIC boundary condition is fully attributable to atmospheric CO_2 since the transient DIC boundary condition was created by using the GLODAPv2 climatological preindustrial DIC and time evolving anthropogenic carbon fields

(transient steady-state approach and the anthropogenic CO_2 fields of Sabine et al. (2004) as described in Desmet et al. 2022). There is no contribution associated with interannual variability since there is no interannual variability in the first place. However, since the anthropogenic contribution is not fully linear there is a slight modulation once the linear trend is removed for the Cons simulation (Figure 6).

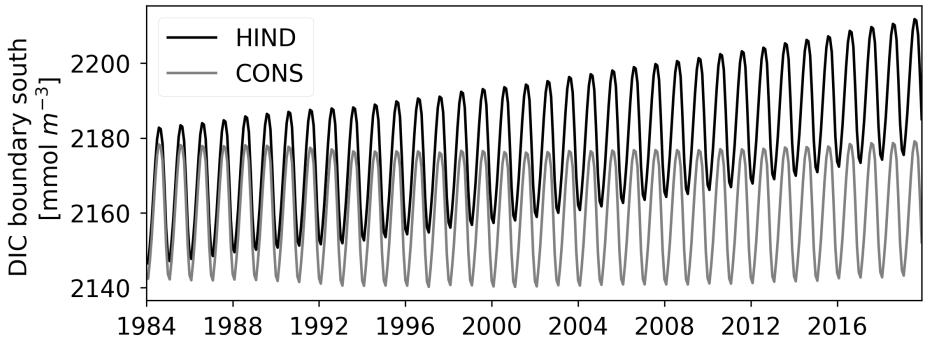

Figure 6: DIC concentration (in mmol m^{-3}) at the southern boundary condition in the case of the HCast (black, HIND) and CCons (grey,CONS) simulations.

In the methods of the revised manuscript, we increased clarity with regard to the absence of interannual variability in the transient DIC concentration of the southern boundary as follows:

Line 112: "The first one corresponds to the simulation used by Desmet et al. [2022] and consists of a hindcast simulation (HCast) from 1979 through 2019, where atmospheric pCO_2 is prescribed to increase according to observations [Landschützer et al., 2020], and where the DIC concentration at the lateral southern open boundary of the model is transient, but does not include interannual variability."

3) In the context of relative threshold, fixed baseline stressor detection, the authors highlight the importance of the ratio of the long-term trend to local variability in determining OAX increase. Could they also shed light on whether temporal changes in the variability contribute? For instance, does the magnitude of variability increase in some regions? This is addressed to an extent by Figure B4, but I find the histograms difficult to interpret due to their small size.

Authors: We thank the reviewer for those interesting questions and comments. From 1984 to 2019, the magnitude of the variability of $[H^+]$ (annual standard deviation) increases in all surface regions and in the subsurface of the CCS, ONP and CNP regions in the HCast simulation (Figure 7). We agree with the reviewer that it would be interesting to shed light on the contribution of those temporal changes in $[H^+]$ variability to the increase in OAX. However, some of those changes in $[H^+]$ variability also occur in the CCons simulation, e.g., the increase in the ONP 100-250 m depth layer (Figure 7). The simulated changes in variability are therefore not only driven by the increase in atmospheric CO_2, but can also be driven by decadal climate modes or climate change feedback such as changes in temperature, etc. Based on the two available simulations, it is therefore not trivial to thoroughly attribute the contribution of the trend in $[H^+]$ versus the variability change to OAX increase.
Yet, we estimated for regions with Gaussian $[H^+]$ distributions (e.g., at 100 m depth of P_{CCS}), i.e., under the assumption of a Gaussian distribution, that the change in variability would only lead to a 1.3 fold increase in OAX days versus a 14-fold increase from the change in mean state (long-term trend). Similarly, it would only lead to a 2% increase in the maximum OAXs intensity versus a 82% increase from the change in mean state.

In order to shed light on whether temporal changes in the variability occur and whether they contribute to OAX increase, we added Figure 7 below to the appendix of the revised manuscript. In the discussion of the revised manuscript, we further discuss those questions in a newly added paragraph as follows:

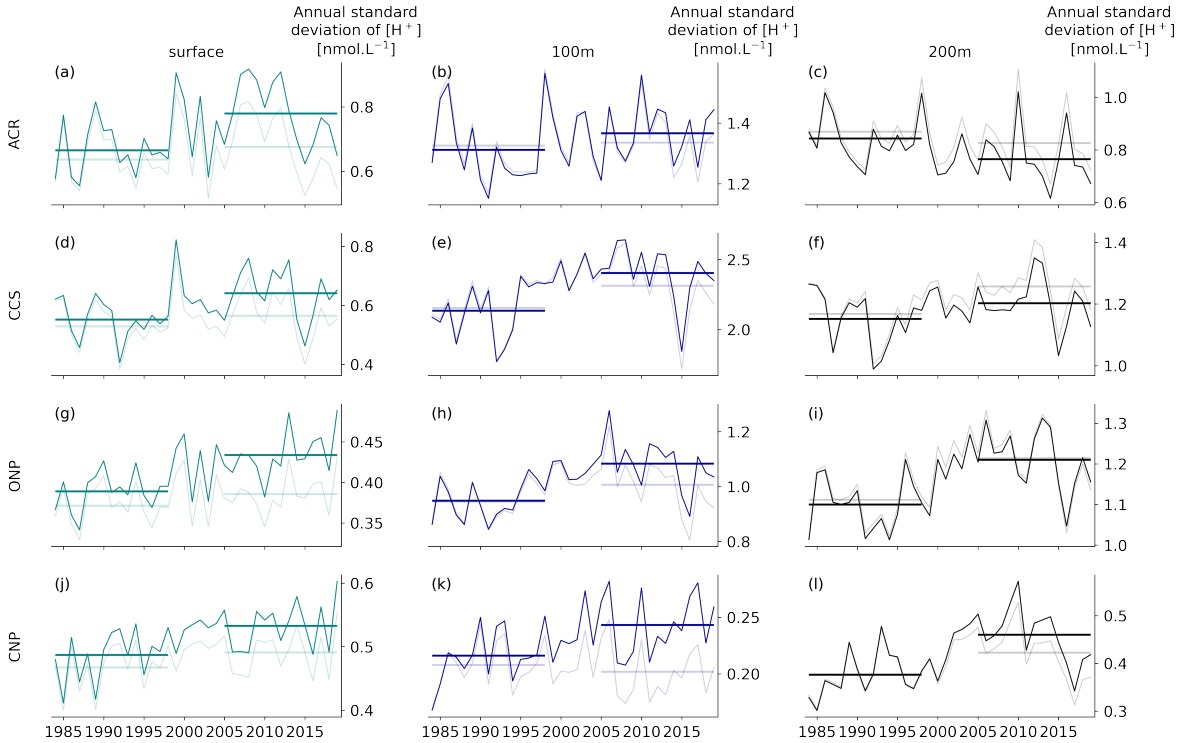

Figure 7: Changes in annual standard deviation of $[H^+]$ in the HCast (dark) and CCons (light) simulations for the four regions (rows) and three depth layers (columns). The horizontal lines depict the average standard deviation during the 15 first and last years of the analysis period for each simulation.

Text added:

Lines 388-398: "When using a relative threshold and a fixed baseline to define OAX, the ratio of the long-term trend to local variability is key in determining the increase in OAX. Thus temporal changes in the variability can have a substantial influence on the evolution of the OAX. Such an increase in variability is actually expected as a consequence of ocean acidification [see also Burger et al., 2020], driven by the increase in the hydrogen ion concentration and a higher sensitivity to change. The variability can also change as a consequence of changes in weather and climate. In our simulations, the variability of $[H^+]$ increases in all surface regions and in the subsurface of the CCS, ONP, and CNP regions (Appendix Figure B5). However, these increases in variability tend to contribute comparatively little to the overall increases in the OAX. We can estimate this contribution most easily in the regions where the $[H^+]$ distributions are Gaussian (e.g., at 100 m depth of P_{CCS}). There, the increase in variability increases the number of OAX days by a factor of 1.3, which is an order of magnitude smaller than the impact of the change in the mean state, as this leads to a 14-fold increase. Similarly, the maximum OAX intensity would increase by only 2% from the change in variability, versus the intensity increases by 82% from the change in mean state.

Technical corrections

Line 49: please add citation. We thank the reviewer for pointing out that a citation was missing and added the corresponding citation in the revised manuscript (Burger et al., 2020)

Figure 1: Please consider rephrasing "[H+] intensity" to reflect that it is the intensity of high [H+] events. Perhaps something like "[H+] event intensity"
We thank the reviewer for this valuable comment for enhancing the clarity of the manuscript and modified the caption of Figure 1 in the revised manuscript as follows: "OAXs intensity (expressed in

[H+] units [nmol.L-1])"

Line 231: "this horizon shoals by 50 m on average". Is this the average over the whole domain or the coastal areas?
We thank the reviewer for asking the question and pointing out that the message was not clear in the manuscript. It is the average over coastal areas only, and it shoals by 45 m to be more precise. In response to the reviewer question, we increased both precision and clarity by modifying the revised manuscript as follows: Line 246: "[...] shoals by 45 m on average in coastal areas, [...]"

Line 532: Are the units on sigma degrees latitude? We thank the reviewer for the question. Sigma is the standard deviation for Gaussian kernel for the smoothing so units are indeed degrees latitude. We added the units in the revised manuscript.

References

Burger, F. A., J. G. John, and T. L. Frölicher, 2020: Increase in ocean acidity variability and extremes under increasing atmospheric CO2. *Biogeosciences*, 4633–4662, doi:https://doi.org/10.5194/bg-17-4633-2020.

Carton, J. A. and B. S. Giese, 2008: A reanalysis of ocean climate using Simple Ocean Data Assimilation (SODA). *Monthly Weather Review*, **136**, 2999–3017, doi:https://doi.org/10.1175/2007MWR1978.1.

Copernicus Climate Change Service (C3S), 2017: ERA5: Fifth generation of ECMWF atmospheric reanalyses of the global climate. *Copernicus Climate Change Service Climate Data Store (CDS),29/08/2020*.

Desmet, F., N. Gruber, E. E. Köhn, M. Münnich, and M. Vogt, 2022: Tracking the space-time evolution of ocean acidification extremes in the California Current System and Northeast Pacific. *Journal of Geophysical Research: Oceans*, 1–30, doi:10.1029/2021jc018159.

Feely, R. A., C. L. Sabine, J. M. Hernandez-Ayon, D. Ianson, and B. Hales, 2008: Evidence for upwelling of corrosive "acidified" water onto the continental shelf. *Science*, **320**, 1490–2, doi:https://doi.org/10.1126/science.1155676.

Franco, A. C., D. Ianson, T. Ross, R. C. Hamme, A. H. Monahan, J. R. Christian, M. Davelaar, W. K. Johnson, L. A. Miller, M. Robert, and P. D. Tortell, 2021: Anthropogenic and Climatic Contributions to Observed Carbon System Trends in the Northeast Pacific. *Global Biogeochemical Cycles*, **35**, 1–21, doi:10.1029/2020GB006829.

Hersbach, H., B. Bell, P. Berrisford, S. Hirahara, A. Horányi, J. Muñoz-Sabater, J. Nicolas, C. Peubey, R. Radu, D. Schepers, A. Simmons, C. Soci, S. Abdalla, X. Abellan, G. Balsamo, P. Bechtold, G. Biavati, J. Bidlot, M. Bonavita, G. De Chiara, P. Dahlgren, D. Dee, M. Diamantakis, R. Dragani, J. Flemming, R. Forbes, M. Fuentes, A. Geer, L. Haimberger, S. Healy, R. J. Hogan, E. Hólm, M. Janisková, S. Keeley, P. Laloyaux, P. Lopez, C. Lupu, G. Radnoti, P. de Rosnay, I. Rozum, F. Vamborg, S. Villaume, and J. N. Thépaut, 2020: The ERA5 global reanalysis. *Quarterly Journal of the Royal Meteorological Society*, **146**, 1999–2049, doi:https://doi.org/10.1002/qj.3803.

Landschützer, P., G. G. Laruelle, A. Roobaert, and P. Regnier, 2020: A uniform pCO2 climatology combining open and coastal oceans. *Earth System Science Data*, **12**, 2537–2553, doi:https://doi.org/10.5194/essd-12-2537-2020.

Lauvset, S. K., R. M. Key, A. Olsen, S. Van Heuven, A. Velo, X. Lin, C. Schirnick, A. Kozyr, T. Tanhua, M. Hoppema, S. Jutterström, R. Steinfeldt, E. Jeansson, M. Ishii, F. F. Perez, T. Suzuki, and S. Watelet, 2016: A new global interior ocean mapped climatology: The 1° × 1° GLODAP version 2. *Earth System Science Data*, doi:https://doi.org/10.5194/essd-8-325-2016, iSBN: 1866-3591.

Response to reviewer's comments (RC2)
Spatiotemporal heterogeneity in the increase of ocean acidity extremes in the Northeast Pacific

Flora Desmet, Matthias Münnich, and Nicolas Gruber

October 26, 2023

General remarks

First and foremost, we thank the editor and this reviewer for their very supportive and insightful comments on our manuscript. We appreciate the valuable remarks that helped us to significantly improve the quality and clarity of this manuscript.

Many of the reviewer's comments were associated with the comprehensibility of the manuscript regarding the definition of key properties and the matching of numbers between figures and text. In the revised manuscript, we modified some figures and improved the clarity of the text based on the reviewer's comments. Furthermore, we considerably shortened the abstract to focus on the core research messages of the manuscript.

Herein, we provide a summary of each of the reviewer's comments (RC2) in black, followed by our point by point replies in blue and the text added or changed in the revised manuscript in red.

Specific replies

Reply to Reviewer's comments (RC2):

Overview

The manuscript titled "Spatiotemporal heterogeneity in the increase of ocean acidity extremes in the Northeast Pacific" undertook an assessment and quantification of ocean acidity extreme events (OAXs) in the Northeast Pacific region. This was accomplished using a high-resolution regional Earth System Model (ROMS-BEC) building upon prior research (Desmet et al. 2022). The authors comprehensively examined various properties of OAXs in the Northeast Pacific Ocean including their intensity, frequency, duration, and heterogeneities in time and space. By employing the return periods and time of emergence (ToE) framework, they substantially captured in the occurrences of OAXs in depths over the recent 30 years.

The paper is logically organized, and the figure are well-presented. The investigation into OAXs in the Northeast Pacific is particularly interesting and holds substantial value due to utilization of a high-resolution model validated against observations.

Authors: We thank the reviewer for the supportive comments.

Nonetheless, there remain certain questions and comments that require clarification prior to proceeding further consideration of publication.

Authors: Hereinafter we reply to the questions and comments, and show associated changes in the revised manuscript.

Major comments

1) The authors underscored the significance of mesoscale eddies in shaping the spatial heterogeneities of OAXs throughout the manuscript. This phenomenon was enabled by the employment of the high-resolution model (ROMS-BEC model), which resolves the mesoscale eddies and associated processes. Would the distinctive pattern of maximum intensity persist under coarser resolutions? To elucidate the reason for the spatial heterogeneities, I propose conducting the additional simulations using the same model with a coarse resolution. While a comparison with Burger's findings in Earth system model has been made, the models are different, and this evidence is indirect. By comparing outcomes from the coarse resolution experiment using the same simulation parameters, you could substantially bolster the argument for the role of mesoscale eddies in driving OAXs.

Authors: We thank the reviewer for this interesting suggestion. We agree that the resolution difference between the coarse-resolution Earth system model used in Burger et al. [2020] and our high-resolution model makes a direct comparison difficult. However, this issue cannot be overcome by running our model at lower resolution, since we are using a relative threshold to define OAX. As a result, very different OAXs are identified depending on the resolution. This is because the use of a coarse resolution model will result in a narrowing of the distribution of $[H^+]$ values at a given location compared to a high-resolution modeling experiment (as illustrated in Figure 1), in particular in regions where mesoscale processes largely affect the distribution. If the relative threshold from the high resolution experiment is kept to detect OAX in both experiments, only very few events to no event will be detected in the coarser resolution experiment. If the relative thresholds are adjusted based on simulated distributions, then the identified OAXs will be very resolution dependent. This prevents a quantitative and meaningful comparison of events across simulated scales.

When it comes to studying extreme events, we believe that it is paramount to simulate the variability in a manner that is as close as possible to reality, and this is much better achieved with a high-resolution than a low-resolution model.

Furthermore, the high-resolution modeling experiment, by resolving both mesoscale and larger scale processes, allows for differentiating the role of each, which would not be the case if we were to do a coarser resolution experiment. Thus, we consider our conclusion about the importance of mesoscale processes for generating extremes as a robust finding (cf., Desmet et al. [2022]), and a conclusion that cannot be bolstered by comparing the outcome to a low-resolution model.

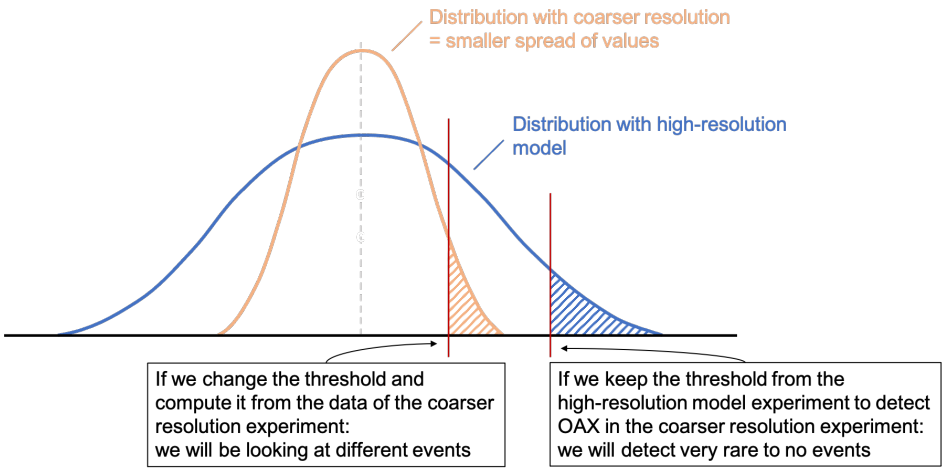

Figure 1: Schematic of two theoretical distributions of $[H^+]$ at a given location from a high-resolution model (blue) and a coarser resolution model (orange). Corresponding theoretical thresholds are plotted in red.

Although the evidence is indirect, i.e., models and parameters are different, findings from Burger et al.

[2020] suggest that the distinctive pattern of maximum intensity found in our manuscript would be different in the coarser resolution study. Indeed, the distinctive pattern of maximum intensity found in our manuscript does not appear in Figure 7d of Burger et al. [2020] (Figure 2), supporting the argument that mesoscale processes are shaping the spatial heterogeneities in OAXs maximum intensity found in our study. Note that besides the difference in model and parameters, the definition of the baseline on which OAXs are detected also differs in the Figure 2 below (i.e., shifting baseline for Figure 2 versus fixed baseline in our manuscript).

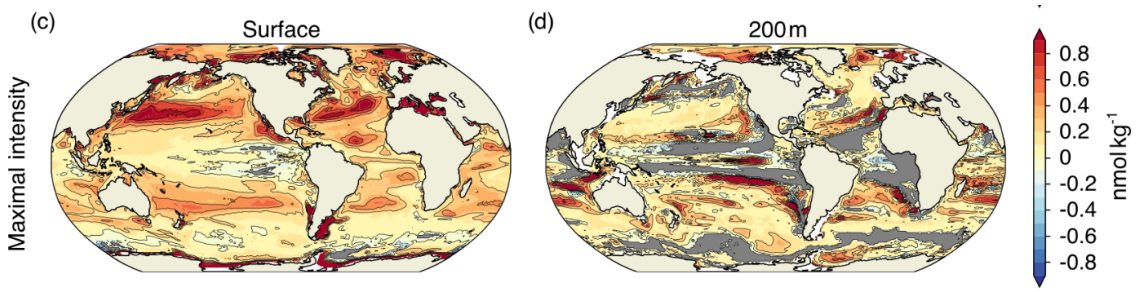

Figure 2: Figure 7 from Burger et al. [2020]: *"Simulated regional changes in [H+] extreme-event characteristics from the preindustrial period to the 2081–2100 period under the RCP8.5 scenario at the surface and at depth for [...] the maximal intensity of events (c, d) [...]. The extreme events are defined with respect to a shifting baseline. Shown are changes averaged over all five ensemble members. Gray colors represent areas where no extremes occur during 2081–2100, and the black lines highlight pattern structures."*

For better clarity, we explicitly stated that the models were different while making the comparison between our findings and Burger et al. [2020]'s findings in the revised manuscript and modified the discussion in section 4.1 as follows:

Text added:
Lines 368-377: "[...] Despite different models used and associated distinct resolutions, the surface increase rates in number of OAX days are similar between our study (3.7 days.μ atm^{-1}) and the study by Burger et al. [2020] (cf. Figure 4a in their study). In the subsurface however, the increase rate in number of extreme days and OAX duration largely differs between the two studies. The increase in number of extreme days at 200 m depth is almost three times slower in our study than in Burger et al. [2020] (cf. Figure A1e of their study), and a similar difference is found for OAXs duration [cf. Figure A1c,d in Burger et al., 2020]. In subsurface waters, where mesoscale processes, such as eddies, largely contribute to broaden the distribution of [H^+] (Appendix Figure B6e,f), differences in OAX increase rate are more dependent on the model resolution than at the surface. In our high-resolution eddy-resolving study, broader distributions lead to thresholds more distinct from the mean than in coarser resolution model that do not resolve mesoscale processes. This likely lead to the slower but more realistic subsurface increase in number of OAX days and OAX duration in our study with respect to increasing atmospheric pCO_2."

We increased clarity with regard to the reason for the spatial heterogeneities of the maximum intensity in the revised manuscript by modifying the discussion as follows:

Text added:
Lines 451-454: "The distinctive pattern of subsurface maximum intensity does not appear in the analyses of Burger et al. [2020] (cf. Figure 7d in their manuscript). We also do not expect it to appear, since the resolution of their model is much coarser (horizontal resolution of ~80 km), preventing it from resolving the mesoscale processes that we identify as shaping this spatial heterogeneities in subsurface OAX maximum intensity."

2) While authors use various properties of OAXs, some of these properties require explicit definitions prior to their usage in the manuscript such as volume fraction of OAX, contribution in Fig.2, near-

permanent OAX in Section 3.5, 4.2. Additionally, it's unclear whether the subsurface layers encompass both 100m and 200m or solely the 200m depth. While these undefined properties are conceptually understandable, but it is needed to provide more precise definitions in an academic context. These specific properties would be recommended within the methods or results sections. Additionally, because the manuscript includes substantial number of acronyms employed throughout the manuscript, it could be beneficial to present a comprehensive table listing these acronyms for clarity.

Authors: We thank the reviewer for pointing out that the definition of some of the OAXs properties were missing or unclear.
To enhance clarity, we renamed the yearly volume fraction into an annual mean volume fraction, and clarified the definition of the volume fraction of OAX in the methods of the revised manuscript as follows:

Lines 179-181: "We additionally derive an integrative metric, namely the annual mean volume fraction of OAX (in %; the average fraction of the daily volume of grid cells with $[H^+]$ above the 99^{th} percentile relative to the total volume extending from 0 to 250 m depth) [...]"

We further made sure that the name of this OAX property was consistently used throughout the revised manuscript and consequently changed the label of the y-axis in Figure 2 and 3 of the original manuscript as well as the caption of these figures.

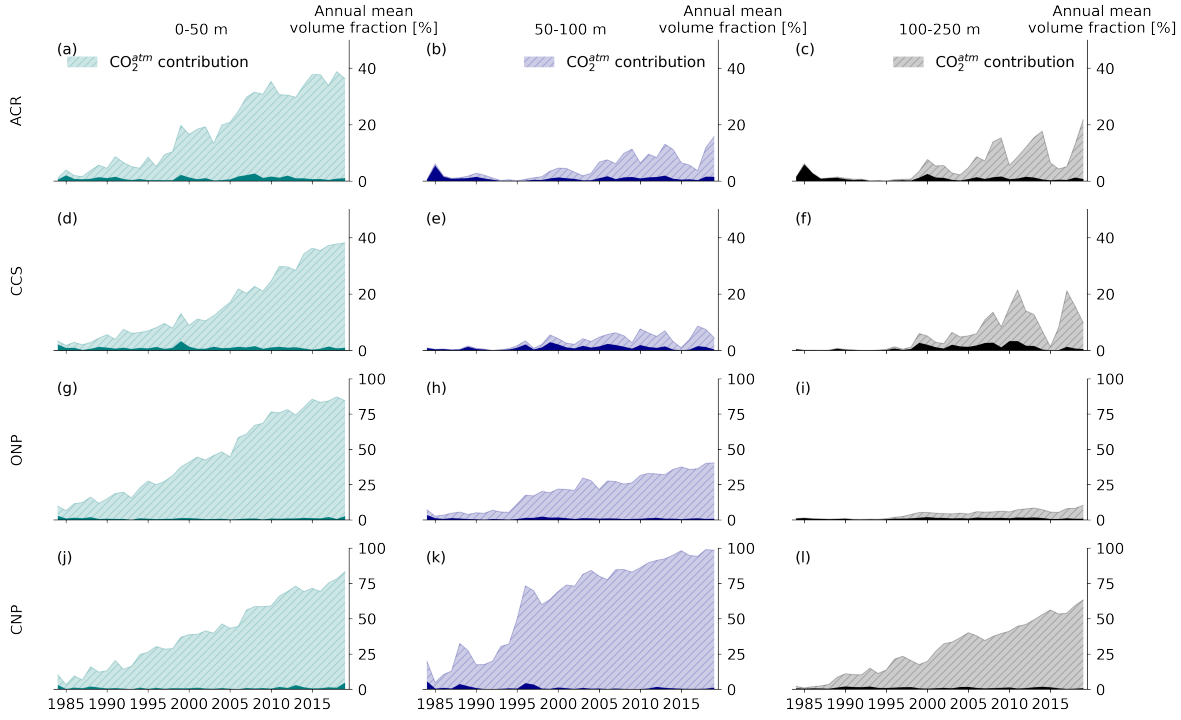

Figure 3: Figure 2 in the original manuscript: Time series of the annual mean volume fraction characterized by $[H^+]$ extremes (OAX) for the four different regions of the Northeast Pacific shown in Figure 1a (rows) and three different depth sections (from left to right: 0-50 m, 50-100 m and 100-250 m depth). Dark and light colours depict the OAX volume fraction in the CCons and HCast scenario, respectively, with the difference between the two denoting the contribution of the rise in atmospheric CO_2 to the OAX volume fraction from the HCast scenario ($CO_2{}^{atm}$ contribution, hatched area). Note the different scales of the top two (0-50%) and bottom two rows (0-100%).

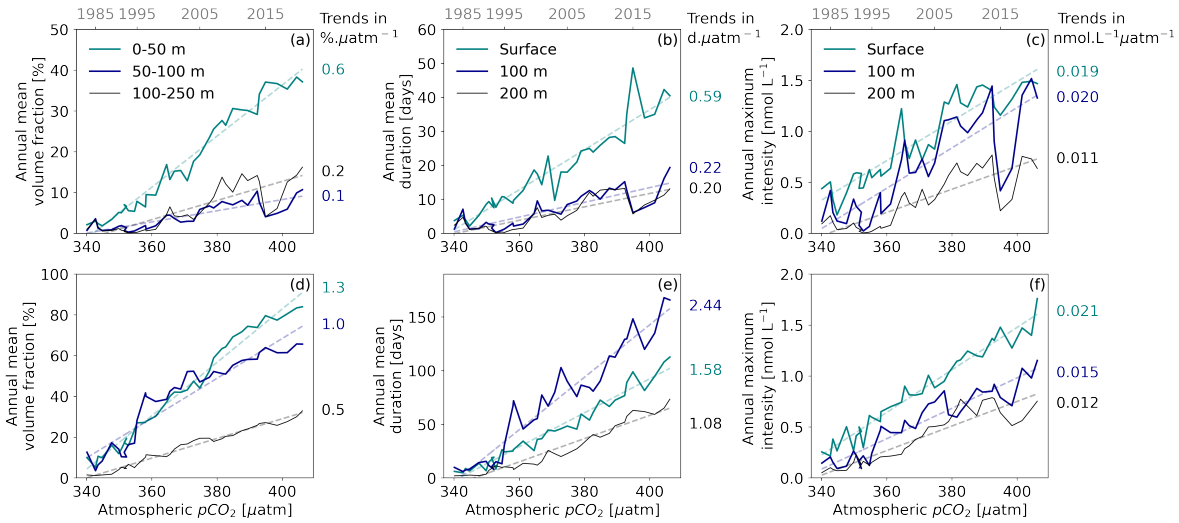

Figure 4: Figure 3 in the original manuscript: OAX characteristics as a function of atmospheric CO_2 between 1984 and 2019 in the (top row) two coastal and (bottom row) two open ocean regions of the Northeast Pacific analysis domain. (a,d) Annual mean OAX volume fraction in three different depth layers (0-50 m, 50-100 m and 100-250 m depth). (b,e) Annual mean event duration (days) and (c,f) annual maximum intensity (nmol L^{-1}) at surface (cyan), 100 m (darkblue) and 200 m (black) depth. In all panels, the simulated OAX characteristics are plotted against the yearly averaged atmospheric pCO_2 over the Northeast Pacific domain. Corresponding years are indicated at the top. Linear regressions ($r^2 > 0.7$) are plotted in each panel and the associated rates of increase (per μatm) are given.

In addition, we explicitly defined the contribution of atmospheric CO_2 to the volume fraction of OAX in the caption of Figure 2 in the original manuscript (Figure 3 in the present letter), and the concept of near permanent OAX in the methods section 2.4 as follows:

Figure 2. [...] Dark and light colours depict the OAX volume fraction in the CCons and HCast scenario, respectively, with the difference between the two denoting the contribution of the rise in atmospheric CO_2 to the OAX volume fraction from the HCast scenario ($CO_2{}^{atm}$ contribution, hatched area). [...]

Text added:

Lines 203-205: "We refer to as "near permanent OAX" when emergence has occurred, i.e., when the linear long-term trend signal has exceeded the 99^{th} percentile threshold used to detect OAX."

Line 354: "The area experiencing near permanent OAX before the end of the hindcast (ToE $<$ 41 years)"

We further made sure that these terms were used consistently throughout the revised manuscript.

We thank the reviewer for pointing out that the definition of the subsurface layers was unclear. We clarified that it encompasses both 100 m and 200 m depth by defining the subsurface layers in the methods of the revised manuscript and we made sure that is was used consistently throughout the text.

Line 176: "These metrics are computed at three depths, i.e., the surface layer in direct interaction with the atmosphere, and two subsurface layers, namely 100 m corresponding to the transition from the euphotic zone to the twilight zone, and 200 m, corresponding to the upper thermocline."

Line 224: while the subsurface (i.e., below 50 m depth) [...]

3) The manuscript employs substantial numbers to elucidate OAX properties. However, the manuscript is inconvenient for matching the numbers with the figures. Consequently, the manuscript is difficult

to follow, and the messages of research can be hindered. For instance, the discussion of Time of Emergence (ToE) is described as 16 years, 25years, 30-32years (L400). However, the ToE years are represented by the year ranging from 1984 to 2020 in figure 7. Authors need to make consistency by providing supplementary for matching ToE explained in the discussion. Similarly in Section 3.2, matching the numbers with figure 3 is also difficult to follow. This issue of mismatching or uncomfortable explanations are abundant through the manuscript. So, the manuscript is needed to enhance its comprehensibility.

Authors: We thank the reviewer for pointing out that the manuscript requires some modifications to enhance its comprehensibility. We increased clarity with regard to matching figures and numbers in the revised manuscript.
For instance, we modified the definition of the ToE in the methods, and the labels of the colorbar in Figure 7 to match the ToE explained in the introduction and the discussion.

Line 199: "We compute the time of emergence (ToE) as a measure of the time it takes for the linear long-term trend signal to exceed the 99th percentile threshold used to detect OAX. [...] We then calculate the number of years after 1979 when this linear trend exceeds the 99th percentile threshold [...]"

Lines 353-360: "The area experiencing near permanent OAX before the end of the hindcast (ToE $\leq$ 41 years) decreases with depth. [...] Both at 100 and 200 m depth, ToE less than $\sim$41 years are confined to the offshore regions that do not have an imprint from coastal variability, i.e., in the CNP west of the eddy front. At P_{CNP}, the ToE is as short as 18 years at 100 m depth, matching [...]"

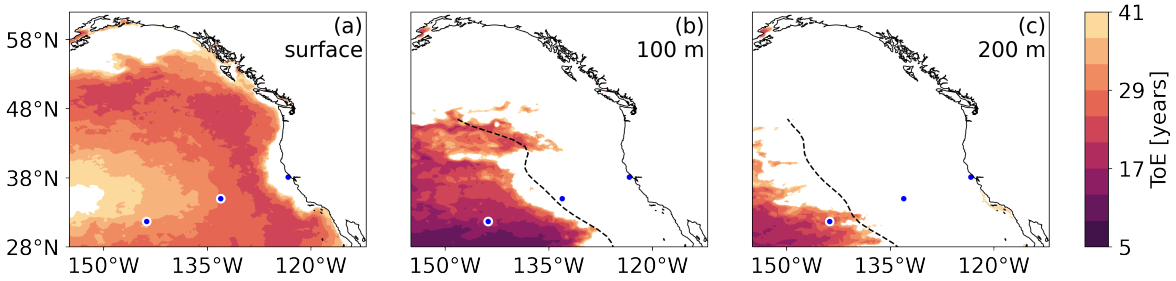

Figure 5: Figure 7 in the original manuscript: Maps of the Time of Emergence (ToE) of the yearly mean $[H^+]$ (long-term trend in $[H^+]$) above the local $[H^+]$ threshold at (a) the surface, (b) 100 m depth, and (c) 200 m depth in the HCast simulation. White areas denote regions where the long-term trend does not exceed the threshold at the end of 2019 (i.e., ToE>41 years). The three blue disks with white contours in each map denote the locations where the time series in Figures 1 and 6 were extracted. The black dashed lines denote the westward eddy propagation fronts.

Additionally, we modified the unit of the trends given in the model evaluation section to match the unit of Table 1 in the revised manuscript, as follows:

Lines 144-152: "The modeled surface pH in the subtropical North Pacific decreases by 0.015 per decade from 1981 to 2011, which is within the range of the observed trend of -0.016 $\pm$ 0.002 decade^{-1} [Lauvset et al., 2015]. The model's trend of -0.016 pH unit decade^{-1} from 1991 to 2011 in the subpolar North Pacific, although overestimated compared to observations, is also within the range of the observed trend of -0.013 $\pm$ 0.005 decade^{-1} [Lauvset et al., 2015]. [...] The average modeled surface pH (Ω_A) trend across the five line P stations is -0.019 decade^{-1} (-0.06 decade^{-1}) against -0.014 decade^{-1} (-0.05 decade^{-1}) in Franco et al. [2021]."

Finally, we enhanced the comprehensibility of the results in Section 3.2 with regard to Figure 3 by adding the linear trends, i.e., the rate of increase, on the revised Figure 3 (see Figure 4 in this response letter) and by modifying the text in the results section as follows:

Lines 259-284:"Near the surface, the increase in OAX volume fraction linearly follows the atmospheric CO_2 rise in both coastal and open ocean regions (r^2 >0.96), with a rate of change in the open ocean regions that is twice as large as that in the coastal regions, [...]. The increase rate decreases substantially below 50 m in the coastal regions [...]. The rate of increase in the open ocean regions is largest at 100 m, being about 50% larger than that at the surface, and more than twice as large as at 200 m. [...] Down to 100 m depth in coastal regions and in the surface of open ocean regions, the intensities increase at nearly the same rate than simulated at the surface of coastal regions. At 200 m depth however, and in the subsurface of open ocean regions, the increase is [...]. By contrasting the above results (Figure 3; HCast simulation) with those from the CCons simulation, [...]"

4) The abstract, while comprehensive, stretches to approximately 550 words, which surpasses the typical length of around 380 words. To effectively encapsulate the core research messages, I recommend shortening the abstract to a more concise form.

Authors: We agree with the reviewer that the abstract needs to be shortened in order to effectively transmit the core research messages of the manuscript. In the revised manuscript, we shortened the abstract from approximately 550 words to 370 words, as follows:

The acidification of the ocean (OA) increases the frequency and intensity of ocean acidity extreme events (OAXs), but this increase is not occurring homogeneously in time and space. Here we use daily output from a hindcast simulation with a high-resolution regional ocean model coupled to a biogeochemical-ecosystem model (ROMS-BEC) to investigate this heterogeneity in the progression of OAX in the upper 250 m of the Northeast Pacific from 1984 to 2019. OAX are defined using a relative threshold approach and using a fixed baseline. Concretely, conditions are considered extreme when the hydrogen ion concentration ($[H^+]$) exceeds the 99^{th} percentile of its distribution in the baseline simulation where atmospheric CO_2 was held at its 1979 level. Within the 36 years of our hindcast simulation, the increase in atmospheric CO_2 causes a strong increase in OAX volume, duration, and intensity throughout the upper 250 m. The increases are most accentuated near the surface, with 88% of the surface area experiencing near permanent extreme conditions in 2019. At the same time, a larger fraction of the OAX become undersaturated with respect to aragonite (Ω_A<1), with some regions experiencing increases up to nearly 50% in their subsurface. There is substantial regional heterogeneity in the progression of OAX, with the fraction of OAX volume across the top 250 m increasing in the Central Northeast Pacific up to 160-times, while the deeper layers of the nearshore regions experience "only" a 4-fold increase. Throughout the upper 50 m of the Northeast Pacific, OAXs increase relatively linearly with time, but sudden rapid increases in yearly extreme days are simulated to occur in the thermocline of the far offshore regions of the Central Northeast Pacific. These differences largely emerge from the spatial heterogeneity in the local $[H^+]$ variability. The limited offshore reach of offshore propagating mesoscale eddies, that are an important driver of subsurface OAX in the Northeast Pacific, causes a sharp transition in the increase of OAX between the rather variable thermocline waters of nearshore regions and the very invariant waters of the Central Northeast Pacific. The spatially and temporal heterogeneous increases in OAX, including the abrupt appearance of near permanent extremes, likely have negative effects on the ability of marine organisms to adapt to the progression of OA and its associated extremes.

Minor comments

L152: What about the mean biases in the spatial patterns of pH and OmegaA? Comparing these biases with data from the Global Ocean Data Analysis Project (GLODAP) could provide the better information for model validation.

Authors: We thank the reviewer for this important question. As stated in the original manuscript (Lines 136-138), for the evaluation of the mean biases in the spatial patterns of pH and Ω_A we refer the reviewer to Desmet et al. [2022], where the model representation of mean conditions in pH and Ω_A has been evaluated, including against GLODAPv2. The HCast simulation in our manuscript uses the same model configuration and forcing as employed by Desmet et al. [2022]. There were some small changes owing to our use of slightly different initial conditions as a result of a change in the forcing

used for the model spin up. While Desmet et al. [2022] used daily fields from the year 1979 as the forcing for the spin up, we use a normal year forcing (apart from atmospheric CO_2, which is transient). The normal year forcing is created by adding daily anomalies of the year 2001 to the climatological mean surface fields of wind stress, short and long-wave radiations, and freshwater fluxes derived from ERA-5 [Hersbach et al., 2020; Copernicus Climate Change Service (C3S), 2017]. The two simulations are therefore not numerically equivalent, but present very similar evaluation results (cf. Figure 6 and Figures 3 and 4 in response to RC1, and Desmet et al. [2022]).
The evaluation of the mean biases in the modeled spatial patterns of pH and Ω_A against GLODAPv2 for the HCast simulation can be seen in the Figure 6 below. Figure 6 shows that ROMS-BEC captures the large-scale interior distribution of pH and Ω_A in the northeast Pacific and especially the spatial pattern of the depth of the pH=7.9 isosurface and of the aragonite saturation horizon with good fidelity. The simulated depths correlate with a Spearman coefficient of respectively r=0.96 and r=0.94 with the depths derived from the climatological GLODAPv2 1°×1° gridded Ω_A observational product [Lauvset et al., 2016]. The model depth of the pH=7.9 isosurface (saturation horizon) is on average 42m (20 m) shallower than that derived from the observations.

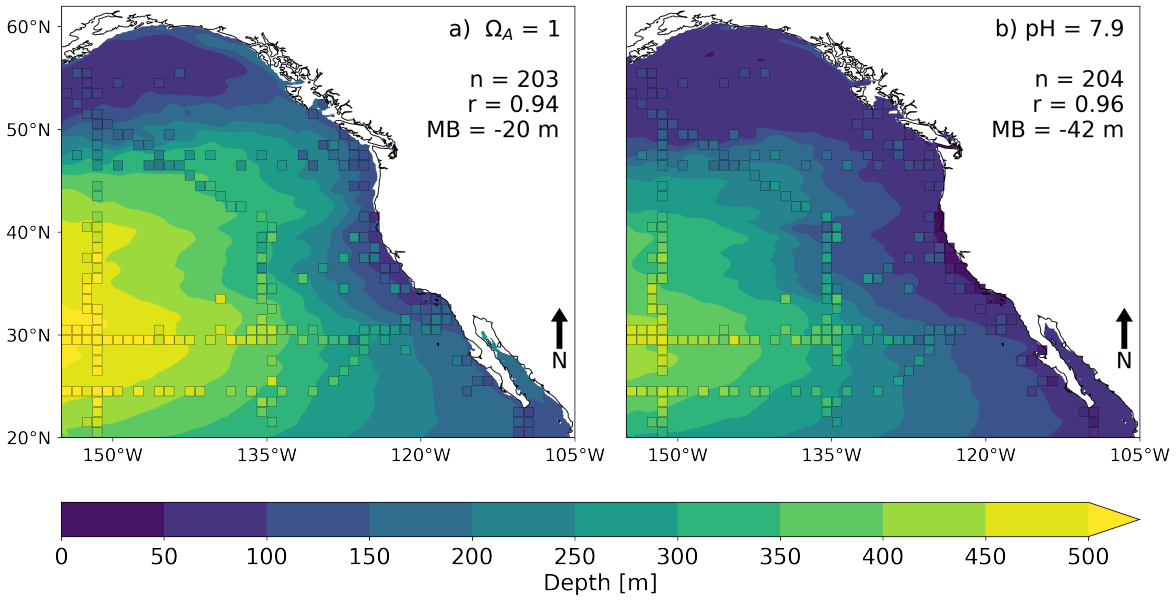

Figure 6: Evaluation of the model (HCast) simulated annual mean depths of (a) the Ω_A saturation horizon ($\Omega_A = 1$) and (b) the pH=7.9 isosurface compared to the corresponding observational estimates based on the 1°× 1° gridded GLODAPv2 climatology [Lauvset et al., 2016]. The model simulated results are shown as filled contours, while the (gridded but not mapped) observations are shown as filled squares. Each square stands for the corresponding 1°× 1° bin of the gridded product. The corresponding spatial Spearman's correlations (r), spatial mean biases (MB), and number of points (n) used for the calculation are indicated at the top.

We address this question by adding the following sentences in the methods of the revised manuscript:

Text added:

Lines 115-120: "Our HCast simulation uses slightly different initial conditions than employed by Desmet et al. [2022] as a result of a change in the forcing used for the model spin up. While Desmet et al. [2022] used daily fields from the year 1979 as the forcing for the spin up, we use a normal year forcing (apart from atmospheric CO_2, which is transient). The normal year forcing is created by adding daily anomalies of the year 2001 to the climatological mean surface fields of wind stress, short and long-wave radiations, and freshwater fluxes derived from ERA-5 [Hersbach et al., 2020; Copernicus Climate Change Service (C3S), 2017]."

Lines 138-140: "Although our HCast simulation is not numerically equivalent to the simulation employed by Desmet et al. [2022] owing to the different initial conditions (cf. Section 2.1), they present very similar evaluation results (not shown). Here we further evaluate the surface OA trends in pH and Ω_A of the model against observations (Table 1)."

L210: The authors mention the strong year-to-year variability and abrupt transition in the subsurface layer. However, there is no explanation of mechanisms for the strong variability and abrupt transition.

Authors: We thank the reviewer for this valuable comment and agree with the reviewer that it is worthwhile exploring the mechanisms for the strong variability and abrupt transition. We shortly discussed the potential mechanisms in the discussion of the original manuscript, but we decided to address those questions in a separate manuscript, in order to not overload the current one. Further investigations of the mechanisms involved in the strong year-to-year and decadal variability can be found in the Chapter 3 of Desmet [2022]. In the revised manuscript we refer to this chapter, and added further explanation in the discussion as follows:

Text added:

Line 405: "While it is beyond the scope of this work to assess the mechanisms driving the strong year-to-year variability in OAXs in the coastal regions (Section 3.1), this variability largely correlates with the El-Niño-Southern-Oscillation, particularly impacting OAX in coastal regions of the Northeast Pacific, as shown in Desmet [2022]."

Line 427: "the occurrence and intensity of OAXs in the CCons simulation correlate with decadal climatic modes such as the North Pacific Gyre Oscillation [Desmet, 2022]."

Line 431: "The timing of the step increases in OAXs in our study may therefore relate to the atmospheric forcing, and would probably vary if we were to run a coupled model, which would have its own decadal and year-to-year variability.

L315: It would be helpful to specify which figure corresponds to the statement being made.

Authors: We agree with the reviewer and specified the corresponding figures in the revised manuscript as follows: Line 331: Figures 2,3,4,5

L326: Also, there is no description of explanation in strongest step increases in subsurface of the CNP, not merely mentioning the occurrence of the strongest step.

Authors: We interpreted this comment as the fact that a discussion on the strongest step increase, found in the subsurface of the CNP and described line 341 in the result section, was missing in the original manuscript. We added the reference to the corresponding Figure in the revised manuscript (Line 341) and discussed more explicitly the reason for this strongest increase in the revised manuscript as follows:

Line 419: "[...], the abruptness of the change also varies spatially, with the strongest step increase in OAX occurring in the subsurface CNP (Section 3.5, Figure 6f).

Line 424: "[...] in low variability regions, such as the subsurface CNP, [...], the non-linearities (step increases) found in those same regions (Section 3.5, Figure 6f) may result from the concurrent effect of OA trends and synergistic low frequency (decadal to multi-decadal) climate variability, as illustrated in Figure 8b"

L357-361: It is advisable to compare the results of Burger et al. 2020 and provide supplementary with similar analysis by using GFDL model results or other Earth system models. Alternatively, if the explanation relies on a specific figure, please indicate which figure elucidates the increase in the number of days as per Burger et al. 2020.

Authors: We thank the reviewer for pointing out that a reference to the specific figure from Burger et al. [2020] used for this comparison was missing. In the revised manuscript, we increased clarity by adding the number of the specific figures from Burger et al. [2020] used to compute the increase rate in number of OAX days and in OAX duration:

L388: It would be helpful to specify which figure corresponds to the statement being made.

Authors: We thank the reviewer for pointing out that clarity could be enhanced by specifying the figures that correspond to the statement made. In the revised manuscript, we increased clarity by dividing Figure 8 into 3 panels (a,b,c) and by specifying that Figure 8c, Figure2h,i and 6e correspond to the statement made as follows:.

Line 417: "This skewness delays the emergence of OA trend over the threshold (e.g., Figure 8c), which explains the weaker increase in OAX (Figures 2h,i and 6e)."

L400, L411: Provide additional details regarding the marine environment, such as temperature, salinity, or other influential factors.

Authors: We thank the reviewer for pointing out that the use of the term marine environment requires to give details about other variables than $[H^+]$, such as temperature or salinity. In the revised manuscript, we were more precise and replaced the term "marine environment" by "ocean carbonate chemistry" (Lines 434 and 445).

L412: How to suggest the emergence of near-permanent OAXs from this figure? A more comprehensive explanation is needed to clarify this point.

Authors: We thank the reviewer for pointing out that the manuscript needs a more comprehensive explanation of how Figure 7 suggests the emergence of near permanent OAXs. As above in response to major comment 2, we explicitly defined the term near permanent OAX in the revised manuscript, in order to increase clarity about this statement. Furthermore, we added a reference to the figure corresponding to the statement made as follows:

Line 447: "(cf. white areas in Figure 7)."

References

Burger, F. A., J. G. John, and T. L. Frölicher, 2020: Increase in ocean acidity variability and extremes under increasing atmospheric CO2. *Biogeosciences*, 4633–4662, doi:https://doi.org/10.5194/bg-17-4633-2020.

Copernicus Climate Change Service (C3S), 2017: ERA5: Fifth generation of ECMWF atmospheric reanalyses of the global climate. *Copernicus Climate Change Service Climate Data Store (CDS),29/08/2020*.

Desmet, F., 2022: *Ocean acidity extremes and their spatiotemporal evolution, a high-resolution modeling study in the northeast Pacific*. Ph.D. thesis, ETH Zürich.
URL `https://doi.org/10.3929/ethz-b-000598701`

Desmet, F., N. Gruber, E. E. Köhn, M. Münnich, and M. Vogt, 2022: Tracking the space-time evolution of ocean acidification extremes in the California Current System and Northeast Pacific. *Journal of Geophysical Research: Oceans*, 1–30, doi:10.1029/2021jc018159.

Franco, A. C., D. Ianson, T. Ross, R. C. Hamme, A. H. Monahan, J. R. Christian, M. Davelaar, W. K. Johnson, L. A. Miller, M. Robert, and P. D. Tortell, 2021: Anthropogenic and Climatic Contributions to Observed Carbon System Trends in the Northeast Pacific. *Global Biogeochemical Cycles*, **35**, 1–21, doi:10.1029/2020GB006829.

Hersbach, H., B. Bell, P. Berrisford, S. Hirahara, A. Horányi, J. Muñoz-Sabater, J. Nicolas, C. Peubey, R. Radu, D. Schepers, A. Simmons, C. Soci, S. Abdalla, X. Abellan, G. Balsamo, P. Bechtold, G. Biavati, J. Bidlot, M. Bonavita, G. De Chiara, P. Dahlgren, D. Dee, M. Diamantakis, R. Dragani, J. Flemming, R. Forbes, M. Fuentes, A. Geer, L. Haimberger, S. Healy, R. J. Hogan, E. Hólm, M. Janisková, S. Keeley, P. Laloyaux, P. Lopez, C. Lupu, G. Radnoti, P. de Rosnay, I. Rozum, F. Vamborg, S. Villaume, and J. N. Thépaut, 2020: The ERA5 global reanalysis. *Quarterly Journal of the Royal Meteorological Society*, **146**, 1999–2049, doi:https://doi.org/10.1002/qj.3803.

Lauvset, S. K., N. Gruber, P. Landschützer, A. Olsen, and J. Tjiputra, 2015: Trends and drivers in global surface ocean pH over the past 3 decades. *Biogeosciences*, **12**, 1285–1298, doi:https://doi.org/10.5194/bg-12-1285-2015.

Lauvset, S. K., R. M. Key, A. Olsen, S. Van Heuven, A. Velo, X. Lin, C. Schirnick, A. Kozyr, T. Tanhua, M. Hoppema, S. Jutterström, R. Steinfeldt, E. Jeansson, M. Ishii, F. F. Perez, T. Suzuki, and S. Watelet, 2016: A new global interior ocean mapped climatology: The 1° × 1° GLODAP version 2. *Earth System Science Data*, doi:https://doi.org/10.5194/essd-8-325-2016, iSBN: 1866-3591.